Supplement of Geosci. Model Dev., 9, 587–606, 2016
http://www.geosci-model-dev.net/9/587/2016/
doi:10.5194/gmd-9-587-2016-supplement

Geoscientific Model Development
Open Access

Supplement of

A global scale mechanistic model of photosynthetic capacity (LUNA V1.0)

A. A. Ali et al.

Correspondence to: C. Xu (xuchongang@gmail.com)

Supplementary Figures

Figure S1 Illustration of the conditional optimization in the LUNA model. In the model, the nitrogen use patterns vary under different environmental conditions. For example, the net photosynthetic carbon gain vs nitrogen allocated to light capture under ambient temperature (mean daytime temperature at 14.75 ^{o}C and mean night time temperature at 11. 45 ^{o}C; blue line) is different from that under the elevated temperature (+5 ^{o}C; red line). Therefore, the net photosynthetic carbon gain under the elevated temperature using optimal nitrogen allocations derived under the elevated temperature (the red point) could be lower than that (the green point) using optimal nitrogen allocations derived under the ambient temperature.

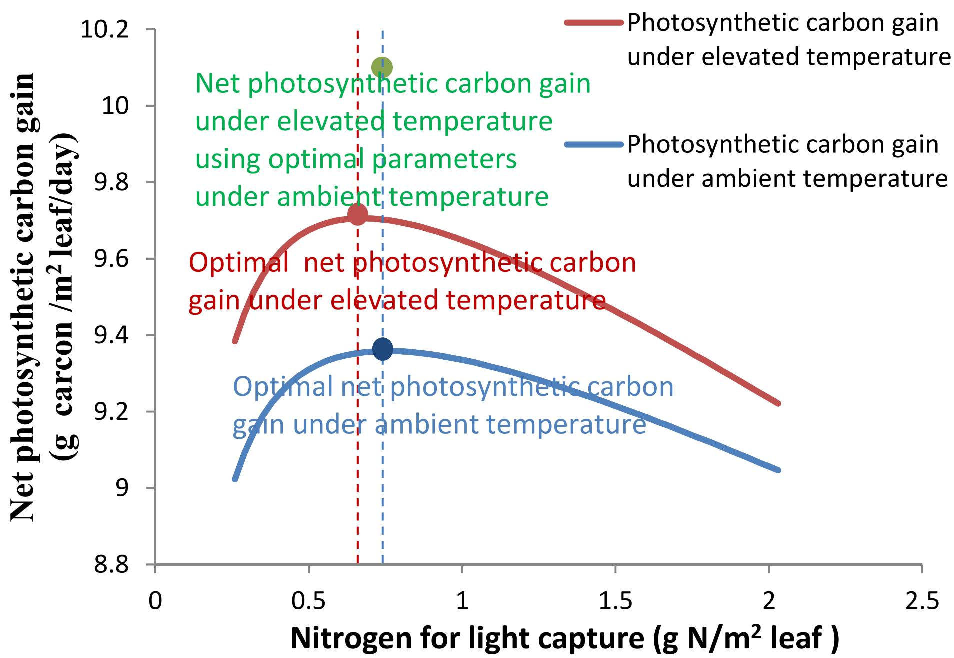

Fig . S2 The spatial distribution map of data used for parameter estimation in LUNA model.

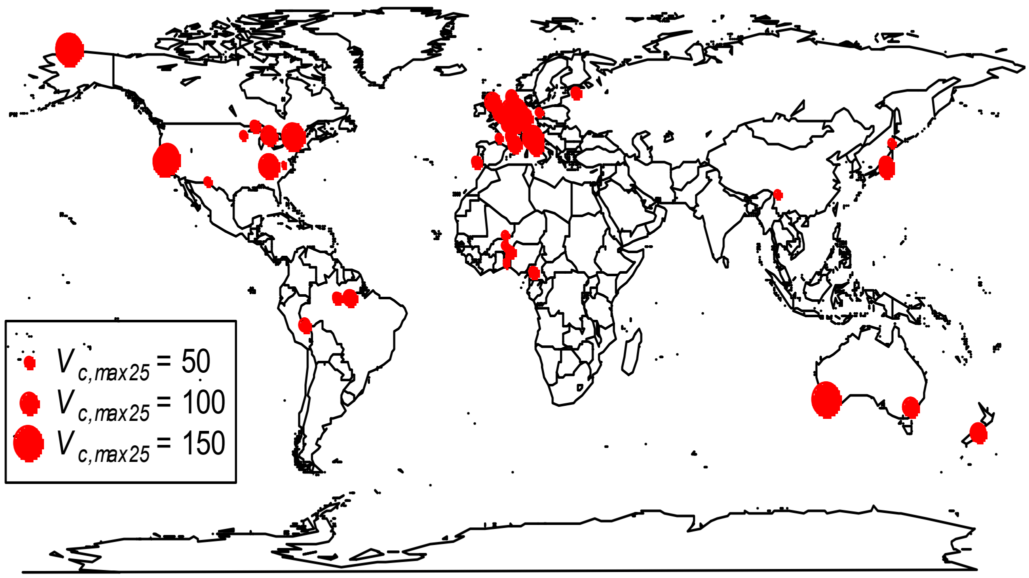

Figure S3 Convergence of parameters obtained by using the Differential Evolution Adaptive Metropolis Snooker updater (DREAM-ZS) sampling technique when TRF1 is used. The parameters include par1: J_{maxb0} (unitless) is the baseline proportion of nitrogen allocated for electron transport rate; par2: J_{maxb1} (unitless) determines the electron transport rate response to light; par3: t_{c,j_0}(unitless) is the baseline ratio of rubisco limited rate to light limited; and par4: H (unitless) determines electron transport rate response to relative humidity. The vertical axis (R_{stat}) represents the deviance of model prediction from observations.

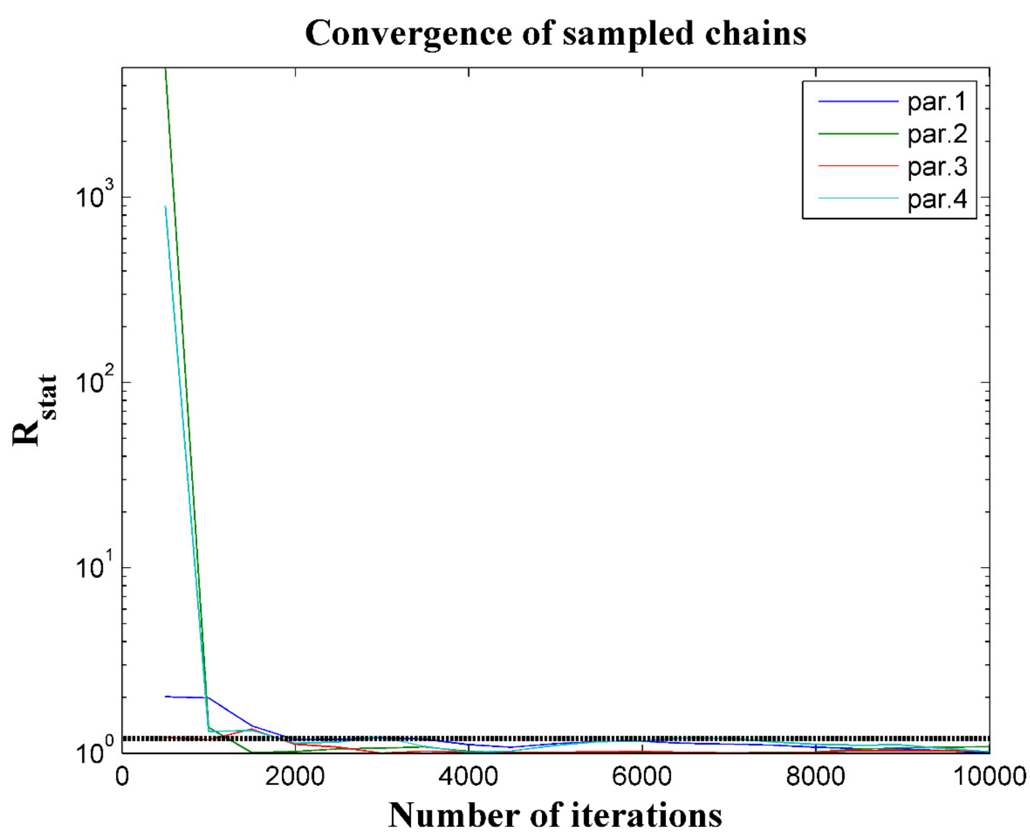

Figure S4 Convergence of parameters obtained by using the Differential Evolution Adaptive Metropolis Snooker updater (DREAM-ZS) sampling technique when TRF2 is used. The parameters include par1: J_{maxb0} (unitless) is the baseline proportion of nitrogen allocated for electron transport rate; par2: J_{maxb1} (unitless) determines the electron transport rate response to light; par3: t_{c,j_0}(unitless) is the baseline ratio of Rubisco limited rate to light limited; and par4: H (unitless) determines electron transport rate response to relative humidity. The vertical axis (R_{stat}) represents the deviance of model prediction from observations.

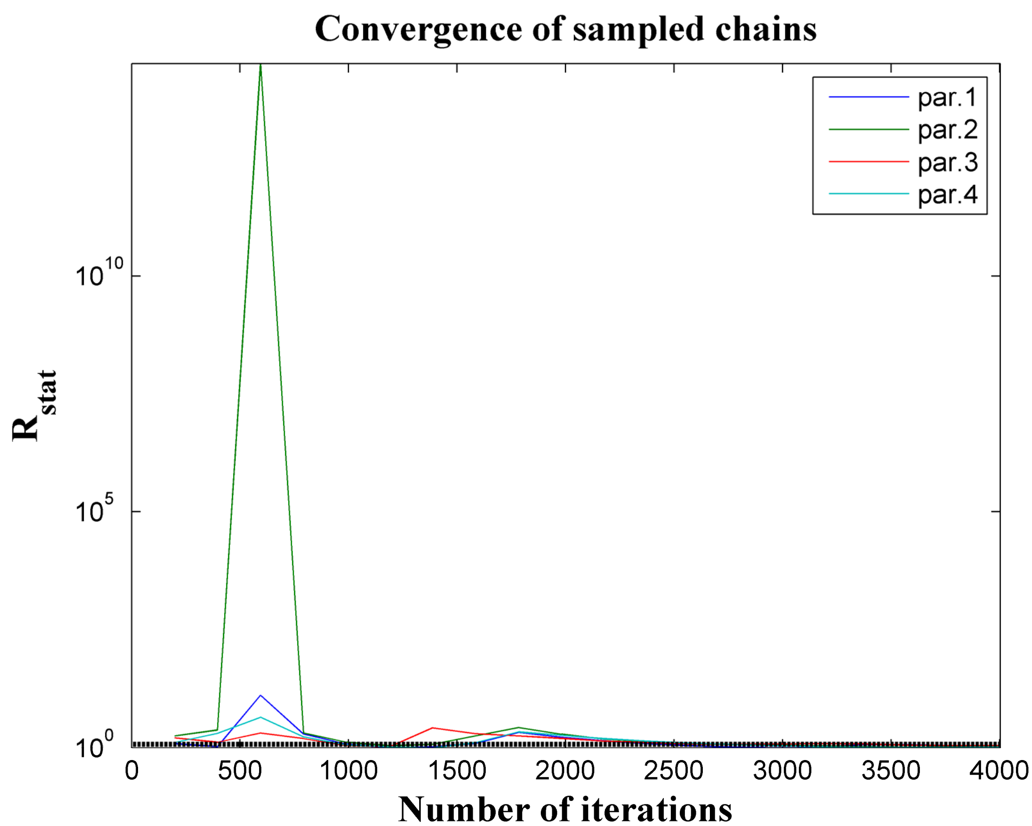

Figure S5 Percentage of variations (r^2 and ME) in observed values of $V_{c,max25}$ (μmol CO_2 m^{-2} s^{-1}) (a: TRF1, c: TRF2) and J_{max25} (μmol electron m^{-2} s^{-1}) (b: TRF1,d: TRF2) explained by the LUAN model across the growing season. All of the studies in the dataset that considered $V_{c,max}$ and J_{max} measurements across the growing season are considered.

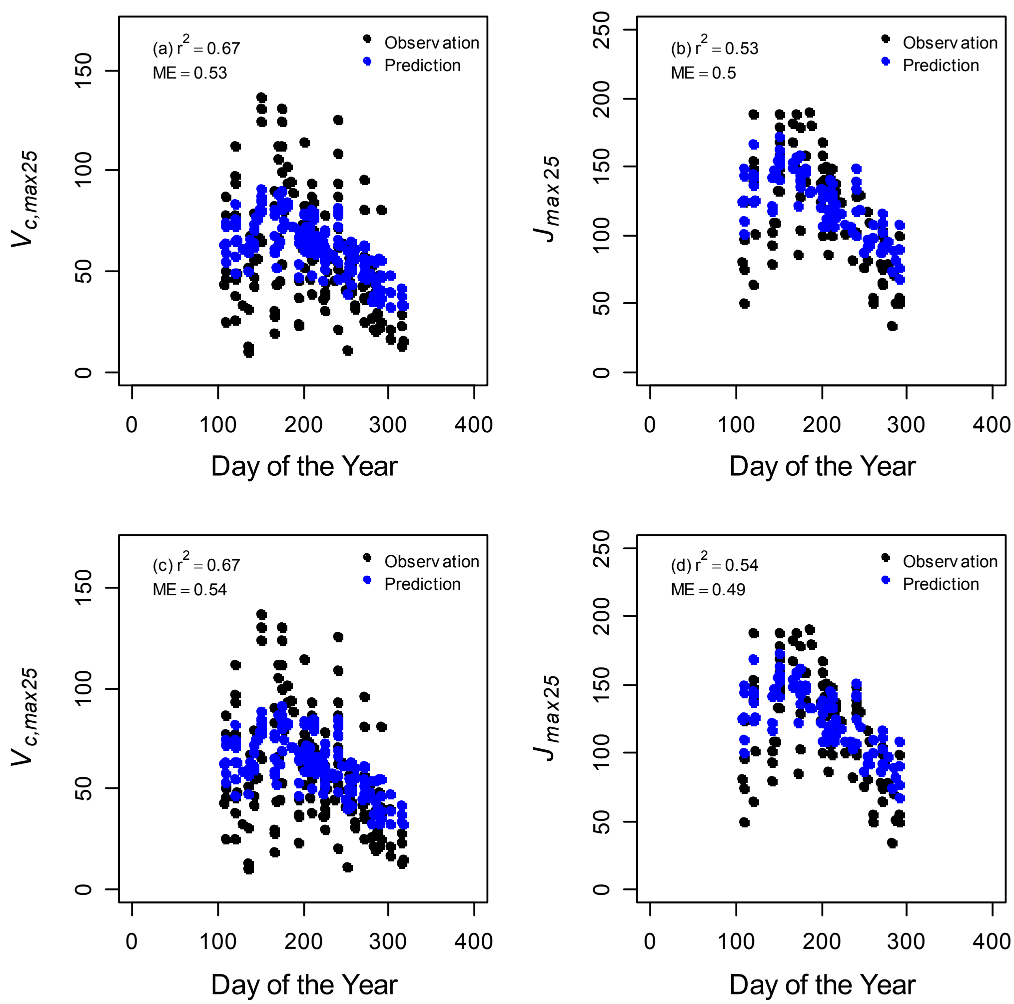

Figure S6 Percentage of variations (r^2 and ME) in observed values of $V_{c,max25}$ (μmol CO_2 m^{-2} s^{-1}) (a:herbaceous, b:shrubs, c:trees)) and J_{max25} (μmol electron m^{-2} s^{-1}) (d: herbaceous, e:shrubs, f: trees) explained by the LUNA model for different plant functional types (PFTs) using TRF1. The dashed line is the 1:1 line between observed and modeled values.

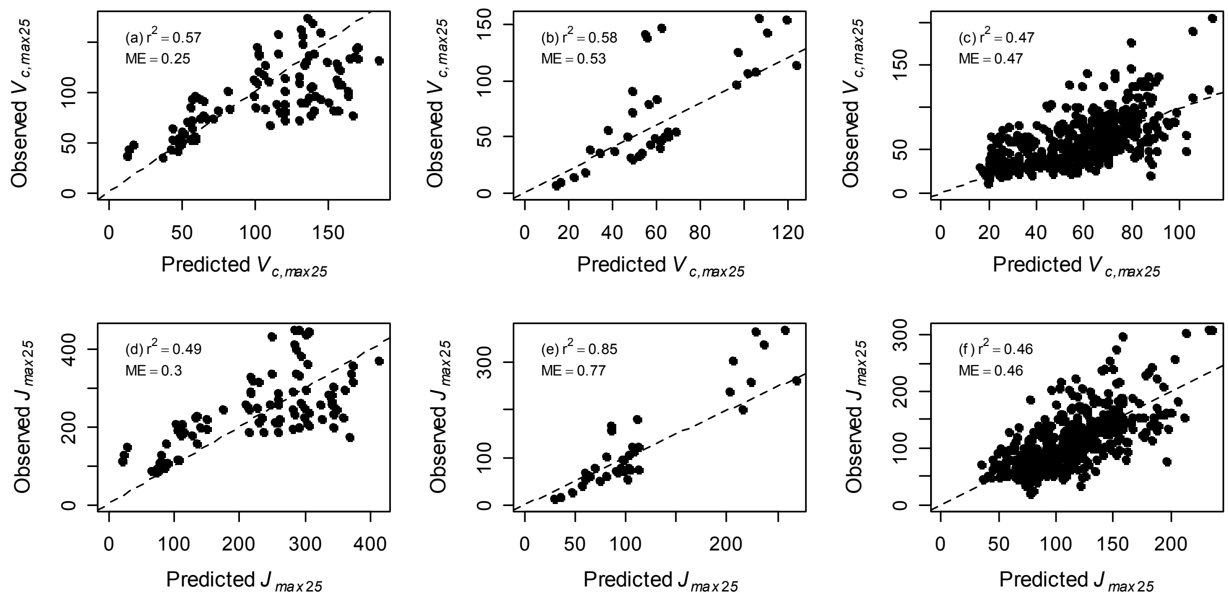

Figure S7 Percentage of variations (r^2, ME) in observed values of $V_{c,max25}$ (μmol CO_2 m^{-2} s^{-1}) (a:herbaceous, b:shrubs, c:trees) and J_{max25} (μmol electron m^{-2} s^{-1}) (d: herbaceous, e:shrubs, f: trees) explained by the LUNA model for different plant functional types using TRF2. TRF2 is a temperature response function that did not consider thermal acclimations. The dashed line is the 1:1 line between observed and modeled values.

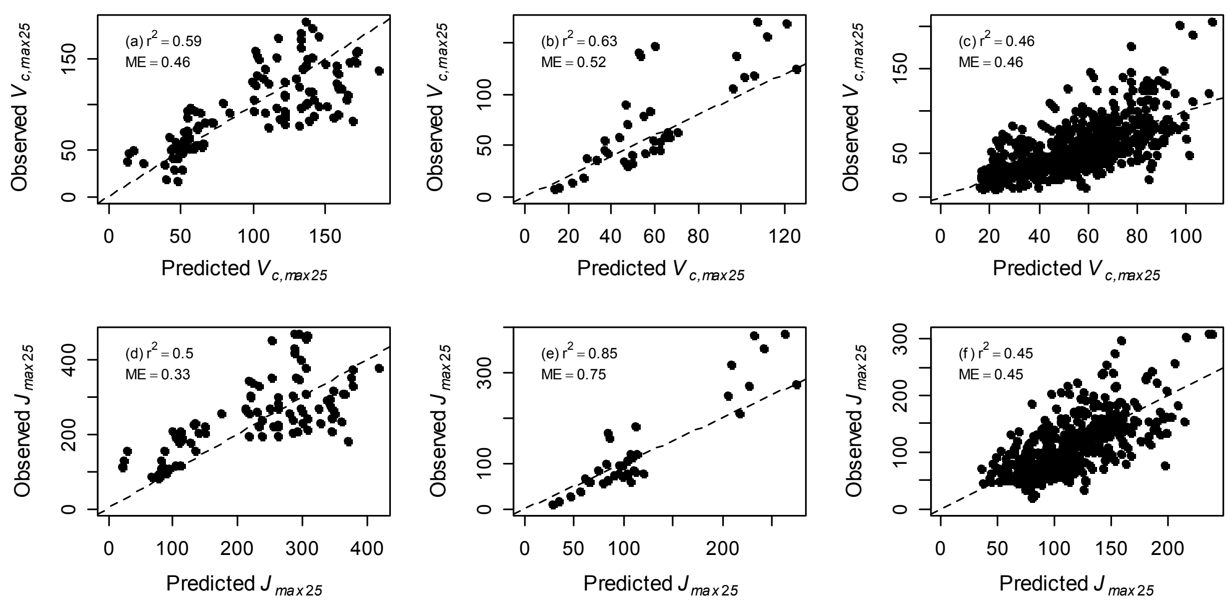

Figure S8 Summer season photosynthetic capacity for the top leaf layer in the canopy including under historical climatic conditions [a: $V_{c,max25}$ (μmol CO_2 m^{-2} s^{-1}), b: J_{max25} (μmol electron m^{-2} s^{-1}] and the difference in either $V_{c,max25}$ (b) or J_{max25} (d) due to changed climatic conditions projected for the future. The difference is calculated by subtracting the photosynthetic capacity predicted by the LUNA model under the historical climate conditions from that under the future climate conditions. The historical climate is represented by the ten-year monthly averages over years 1995-2004 and the future climate is represented by the ten-year monthly averages over years 2090-2099. The model is run by using TRF2, which did not consider the thermal acclimations.

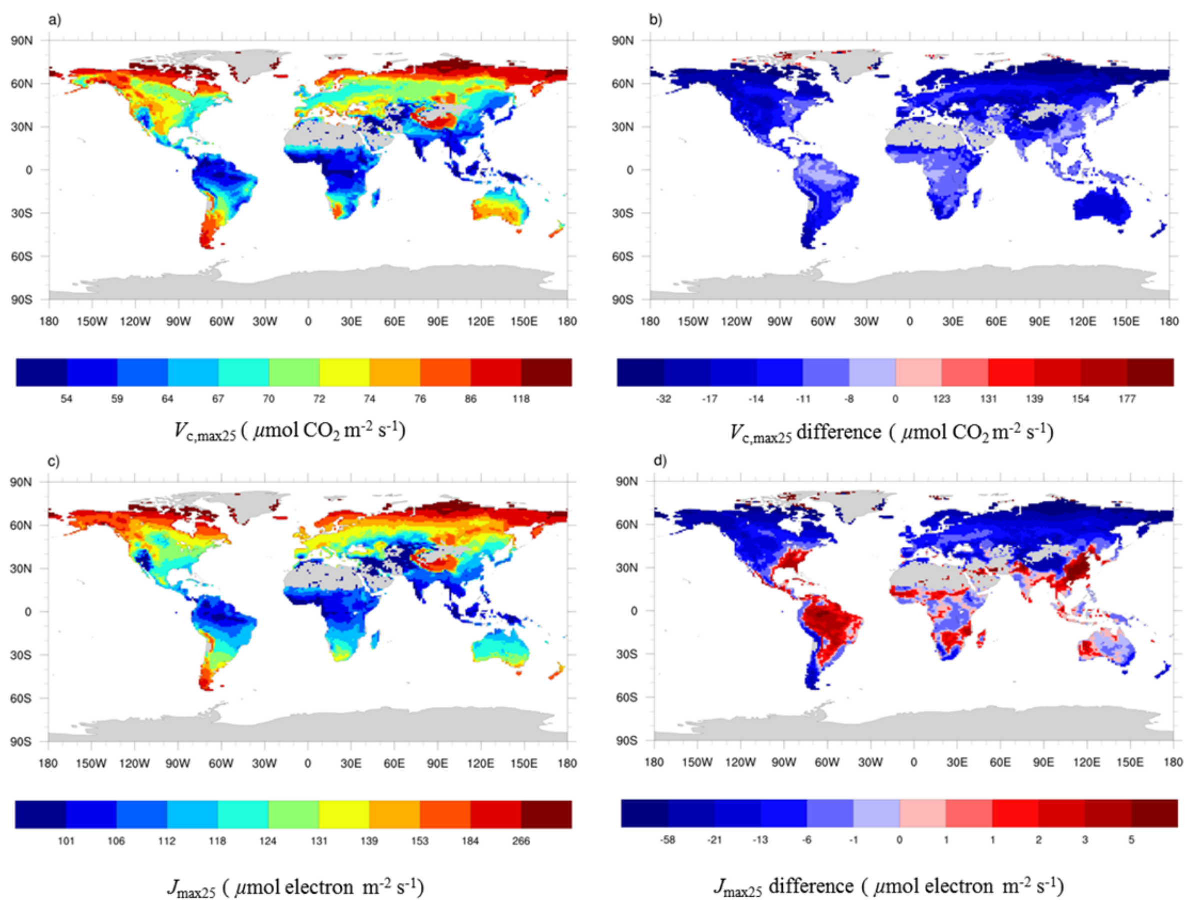

Figure S9 Sensitivity of $V_{c,max25}$ (μmol CO_2 m^{-2} s^{-1}) to projected future changes in environmental variables including temperature (a), radiation (b), humidity (c), and CO_2 (d) across the globe by using TRF2. TRF2 is a temperature response function that did not consider the thermal acclimations. The sensitivity analysis is conducted by changing the value of an individual environmental variable from its 10-year monthly averages in the past (1995-2004) to those in the future (2090-2099) for each individual grid cell across the globe. Positive values indicate that the increase in a specific environmental variable leads to larger values of $V_{c,max25,}$ while negative values indicate that the increase in a specific environmental variable leads to smaller values of $V_{c,max25.}$

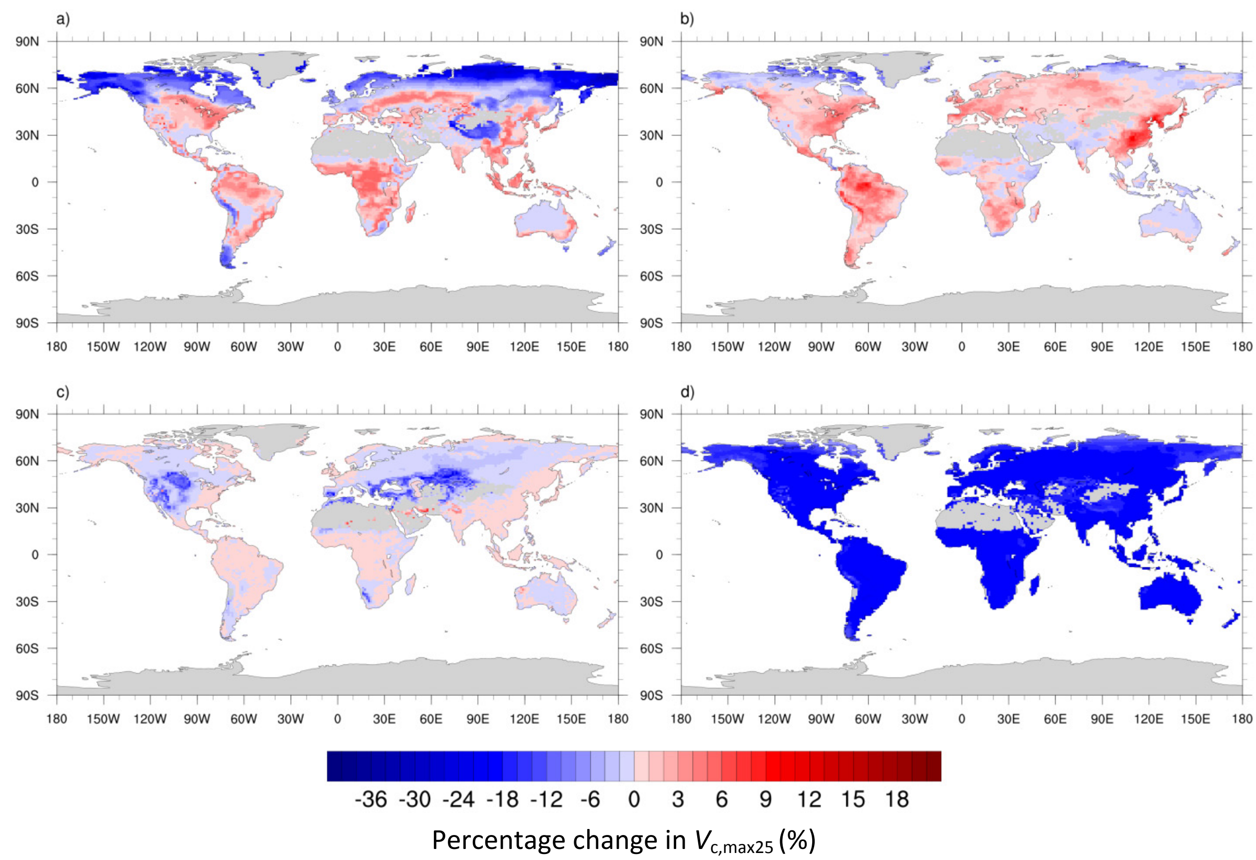

Figure S10 Sensitivity of J_{max25} (μmol electron m^{-2} s^{-1}) to projected future changes in environmental variables including temperature (a), radiation (b), humidity (c), and CO_2 (d) across the globe using TRF2. TRF2 is a temperature response function that did not consider the thermal acclimations. The sensitivity analysis is conducted by changing the value of an individual environmental variable from its 10-year monthly averages in the past (1995-2004) to those in the future (2090-2099) for each individual grid cell across the globe. Positive values indicate that the increase in a specific environmental variable leads to larger values of $V_{c,max25,}$ while negative values indicate that the increase in a specific environmental variable leads to smaller values of $V_{c,max25.}$

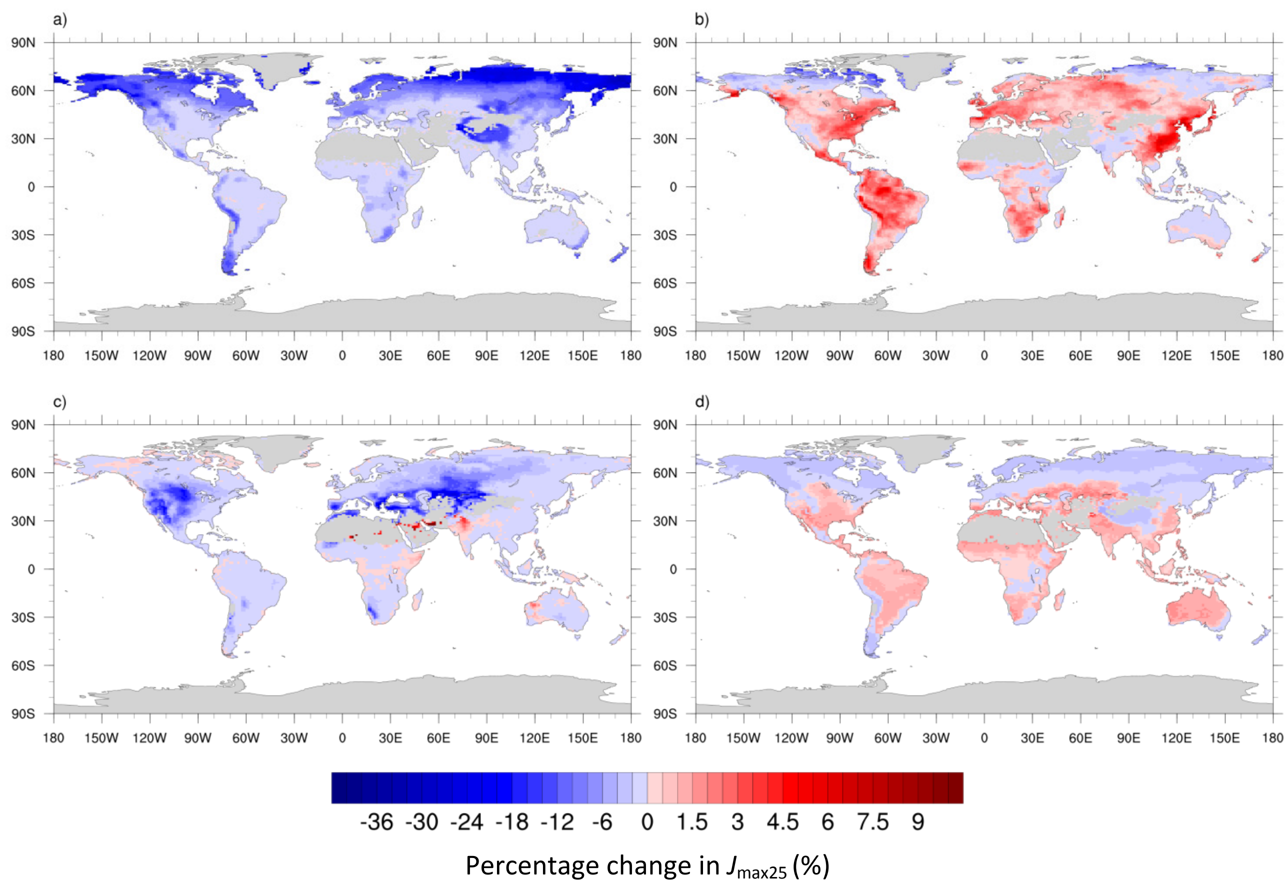

Figure S11 Summer season temperature (°C) under historical (a) and future climatic conditions (b). The historical climate is represented by the ten-year monthly averages over years 1995-2004 and the future climate is represented by the ten-year monthly averages over years 2090-2099.

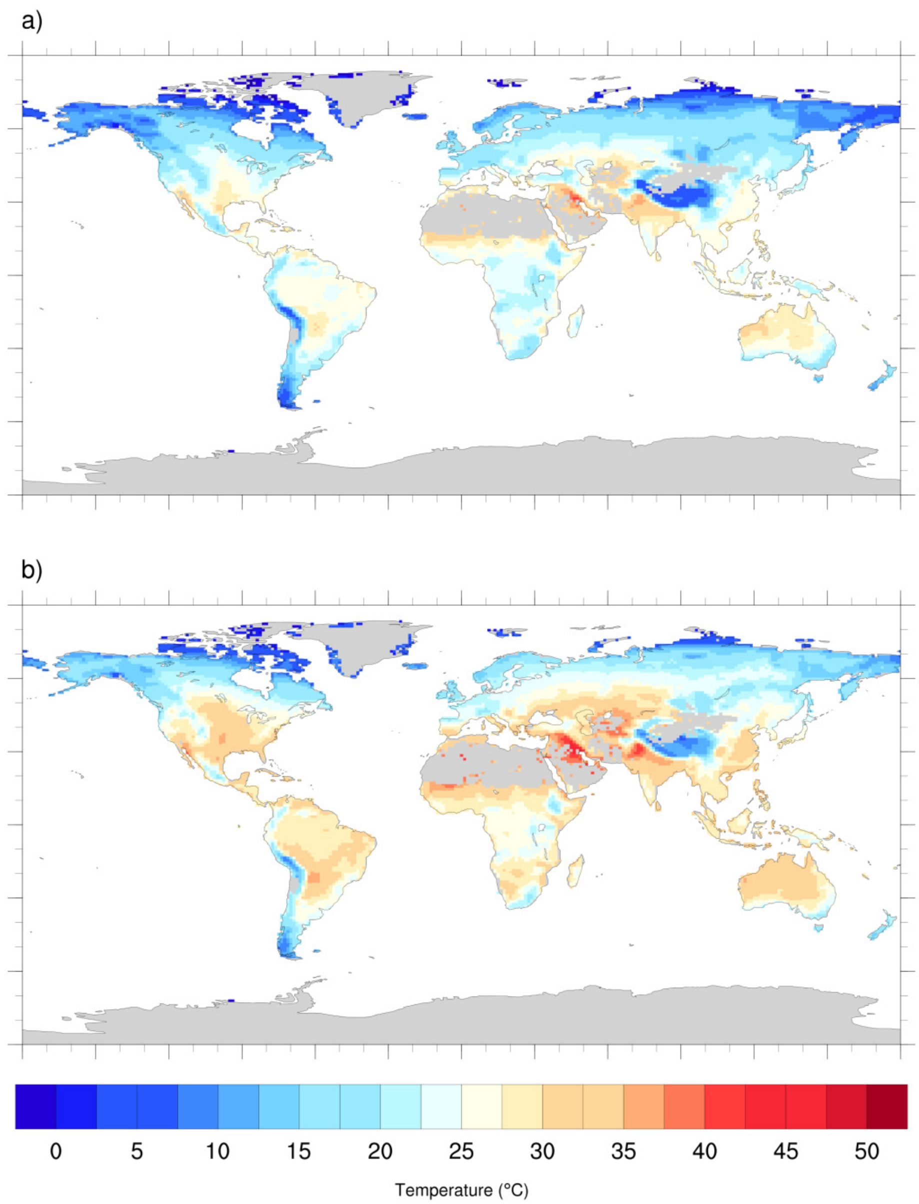

Figure S12 Percentage of variations (r^2 and ME) in observed values of $V_{c,max25}$ (μmol CO_2 m^{-2} s^{-1}) (a: TRF1, c: TRF2) and J_{max25} (μmol electron m^{-2} s^{-1}) (b: TRF1, d: TRF2) explained by a multi-linear regression over leaf nitrogen content (g N/m^2 leaf) and the leaf mass per unit area (g dry mass /m^2 leaf). The dashed line is the 1:1 line between observed and modeled values.

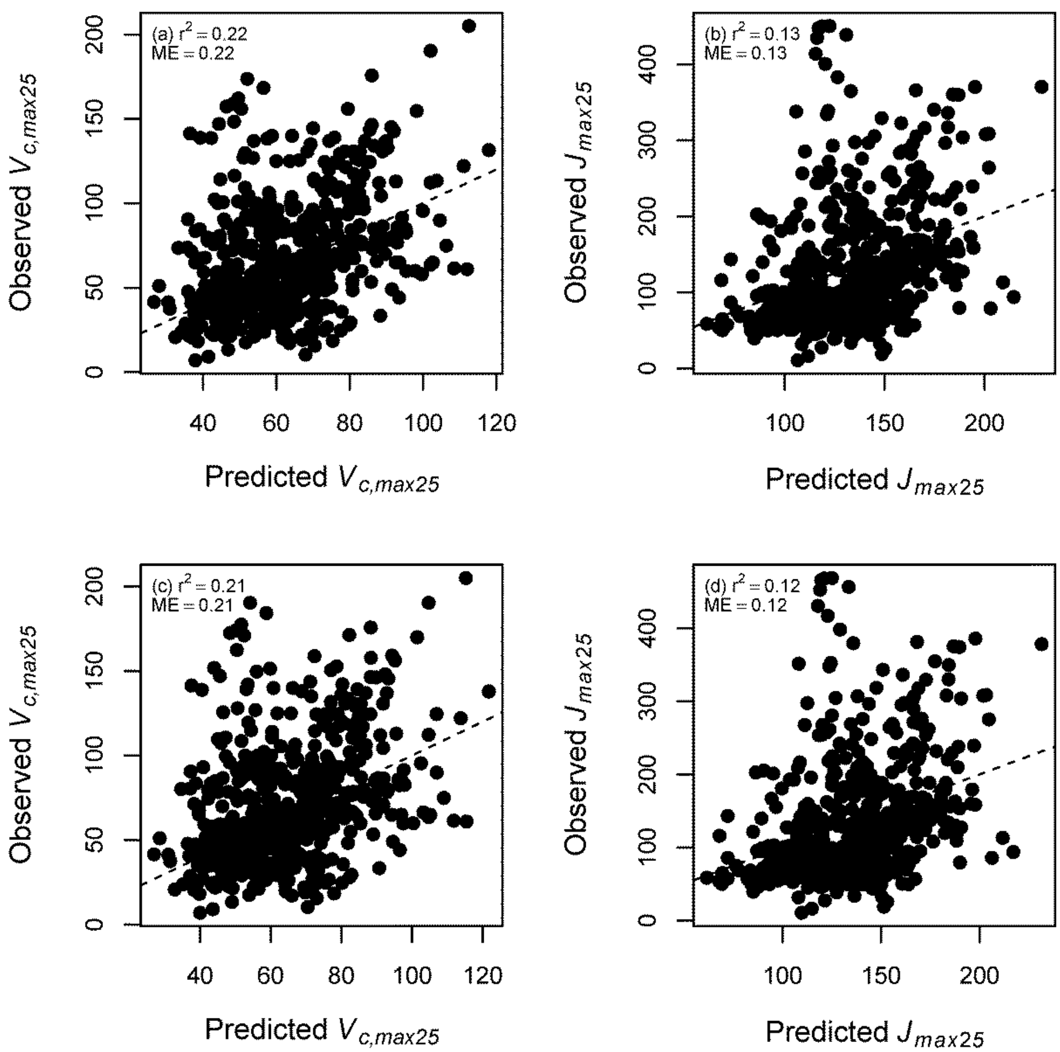

Figure S13 Summer season difference in the temperature (°C) due to changed climatic conditions (temperature under the future climate minus temperature under the historical climate). The historical climate is represented by the ten-year monthly averages over years 1995-2004 and the future climate is represented by the ten-year monthly averages over years 2090-2099.

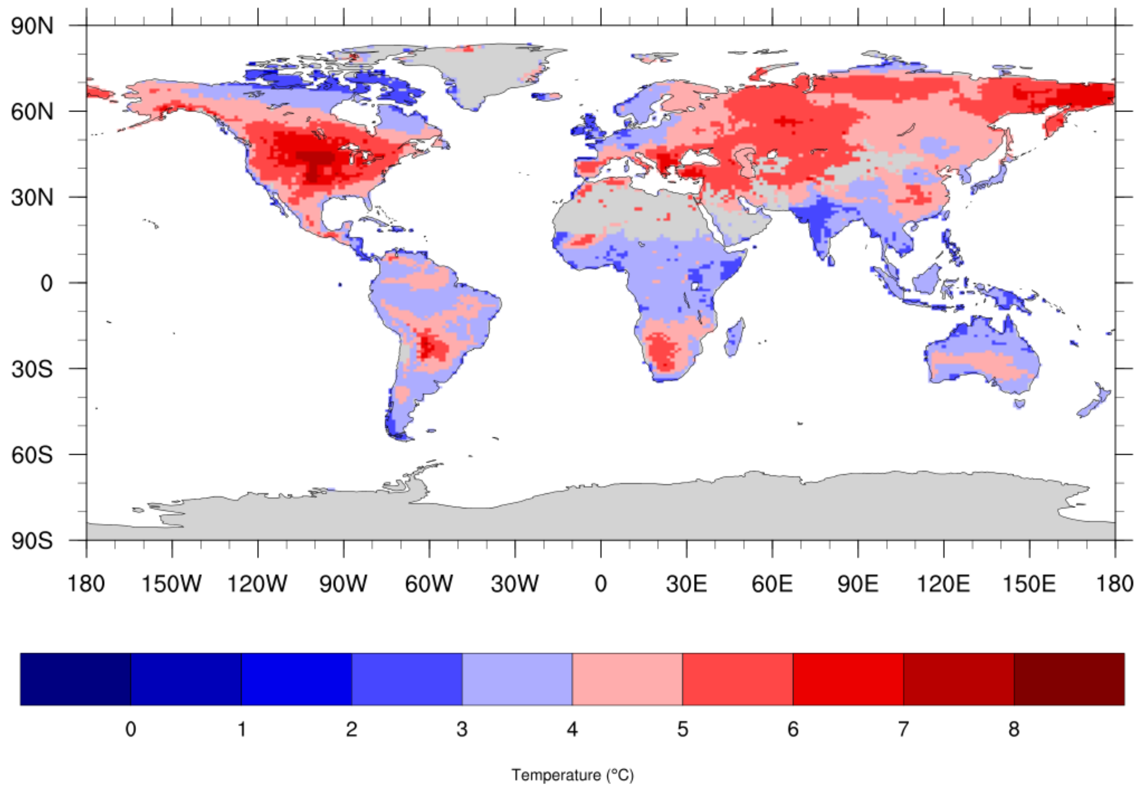

Figure S14 Summer season radiation (Radiation; W m^{-2}) under historical (a) and future climatic conditions (b). The historical climate is represented by the ten-year monthly averages over years 1995-2004 and the future climate is represented by the ten-year monthly averages over years 2090-2099.

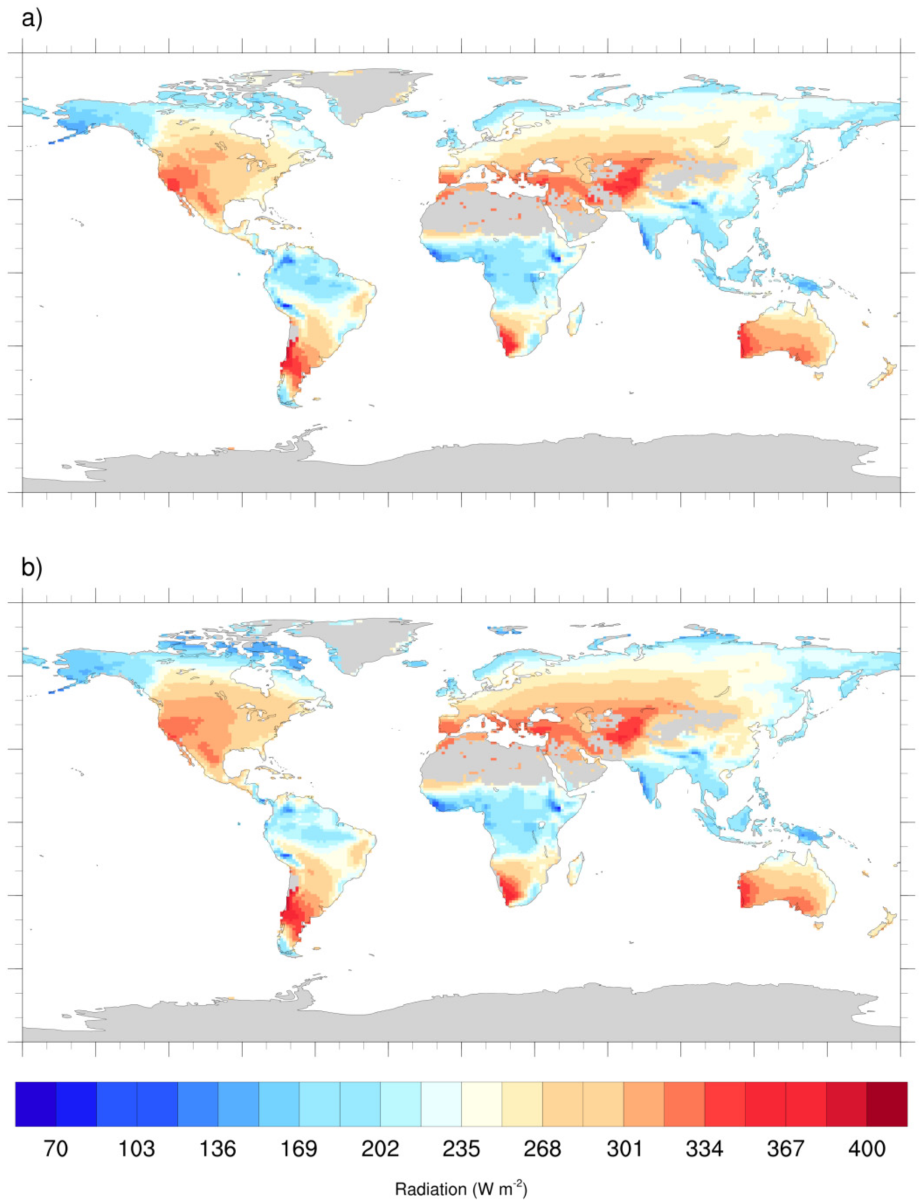

Figure S15 Summer season difference in solar radiation (W m^{-2}) due to changed climatic conditions (radiation under future climate minus radiation under historical climate). The historical climate is represented by the ten-year monthly averages over years 1995-2004 and the future climate is represented by the ten-year monthly averages over years 2090-2099.

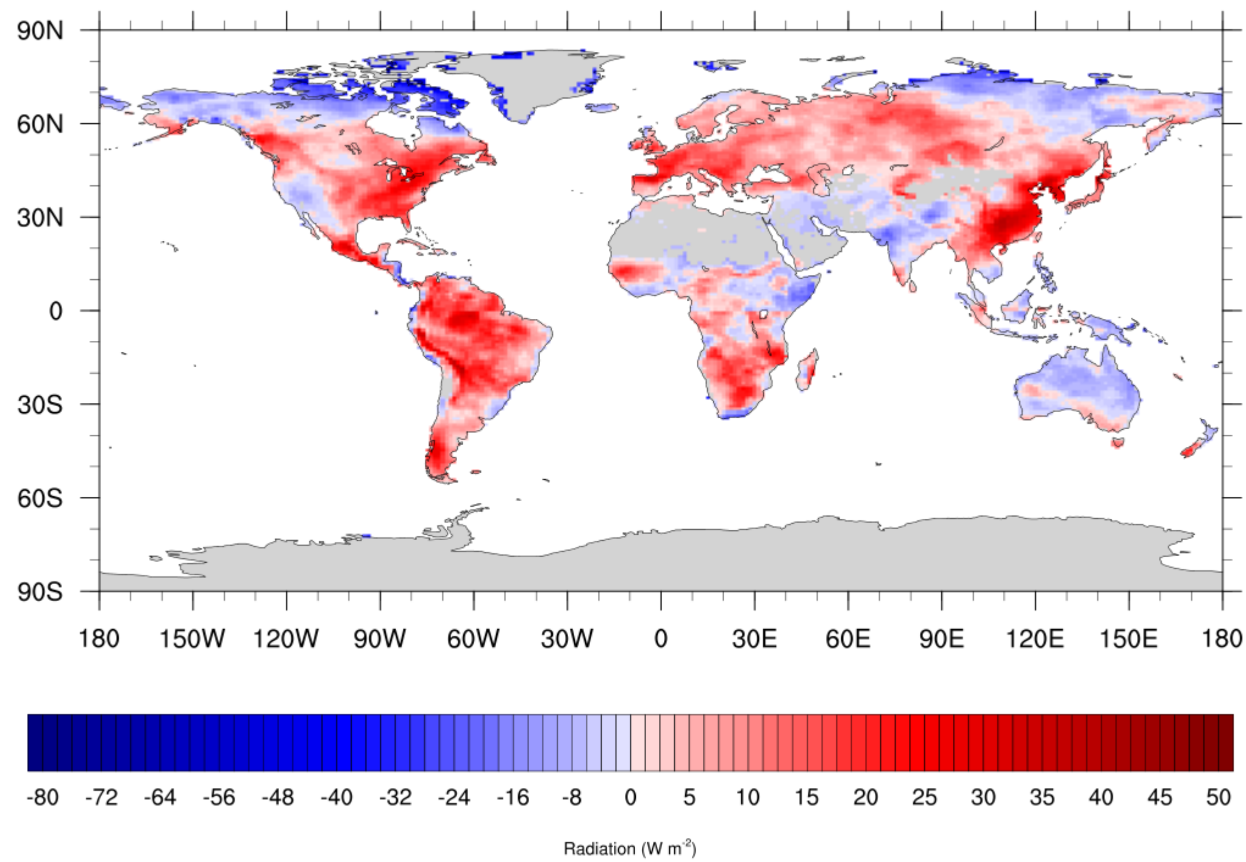

Figure S16 Summer season relative humidity (Relative Humidity; unitless) under historical (a) and future climate conditions (b). The historical climate is represented by the ten-year monthly averages over years 1995-2004 and the future climate is represented by the ten-year monthly averages over years 2090-2099.

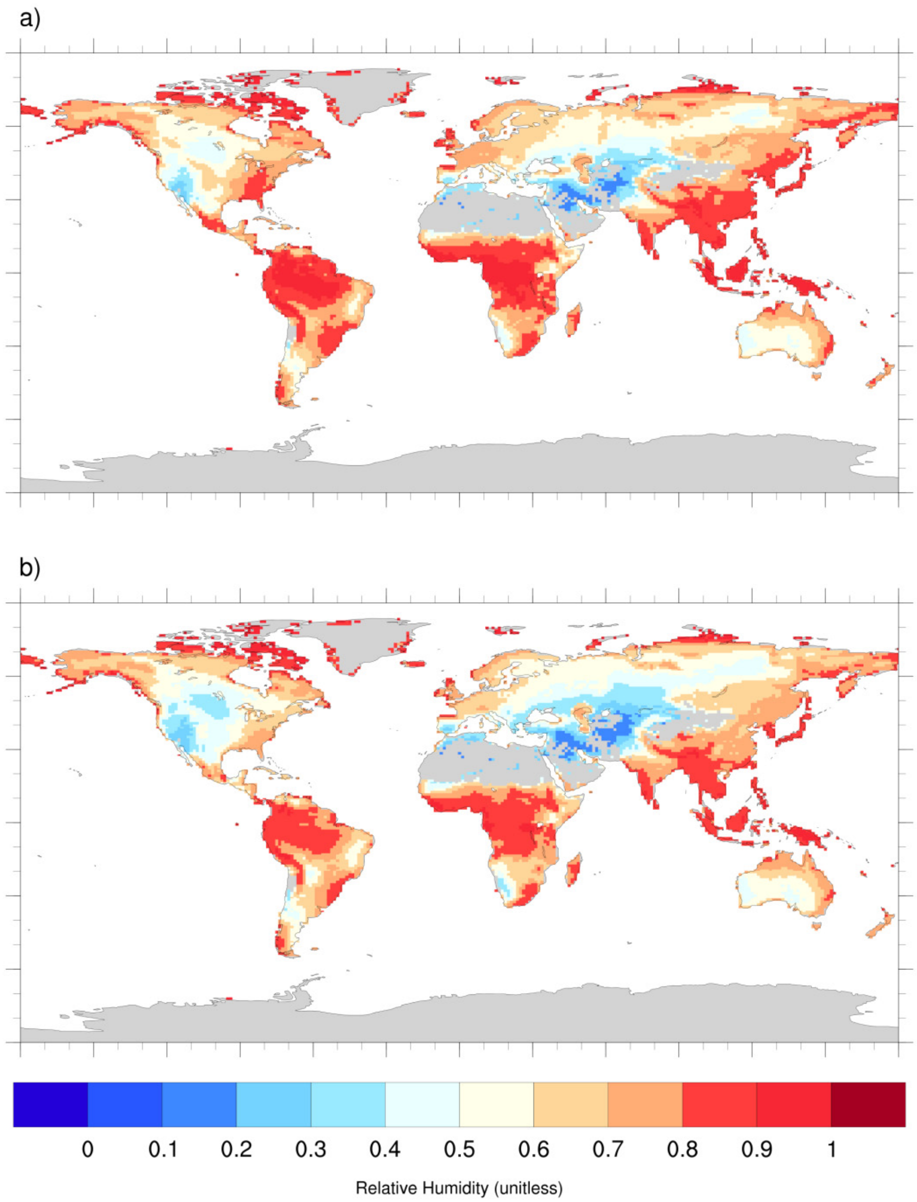

Figure S17 Summer season difference in relative humidity due to changed climate conditions (relative humidity under the future climate minus relative humidity under the historical climate). The historical climate is represented by the ten-year monthly averages over years 1995-2004 and the future climate is represented by the ten-year monthly averages over years 2090-2099.